ARTICLE

ACS chemical biology

Profiling Heparin–Chemokine Interactions Using Synthetic Tools

Jose L. de Paz[†,§], E. Ashley Moseman[‡], Christian Noti[†], Laura Polito[†], Ulrich H. von Andrian[‡], and Peter H. Seeberger[†,*]

[†]Laboratory for Organic Chemistry, Swiss Federal Institute of Technology (ETH) Zürich, Wolfgang-Pauli-Strasse 10, HCI F315, 8093 Zürich, Switzerland and [‡]The Center for Blood Research, Department of Pathology, Harvard Medical School, NRB 836, Boston, Massachusetts 02115, [§]Current address, Grupo de Carbohidratos, Instituto de Investigaciones Químicas, CSIC-USE, Americo Vespucio 49, E-41092, Seville, Spain.

ABSTRACT Glycosaminoglycans (GAGs), such as heparin or heparan sulfate, are required for the *in vivo* function of chemokines. Chemokines play a crucial role in the recruitment of leukocyte subsets to sites of inflammation and lymphocytes trafficking. GAG–chemokine interactions mediate cell migration and determine which leukocyte subsets enter tissues. Identifying the exact GAC sequences that bind to particular chemokines is key to understand chemokine function at the molecular level and develop strategies to interfere with chemokine-mediated processes. Here, we characterize the heparin binding profiles of eight chemokines (CCL21, IL-8, CXCL12, CXCL13, CCL19, CCL25, CCL28, and CXCL16) by employing heparin microarrays containing a small library of synthetic heparin oligosaccharides. The chemokines differ significantly in their interactions with heparin oligosaccharides: While some chemokines, (e.g., CCL21) strongly bind to a hexasaccharide containing the GlcNSO3(6-OSO3)-IdoA(2-OSO3) repeating unit, CCL19 does not bind and CXCL12 binds only weakly. The carbohydrate microarray binding results were validated by surface plasmon resonance experiments. *In vitro* chemotaxis assays revealed that dendrimers coated with the fully sulfated heparin hexasaccharide inhibit lymphocyte migration toward CCL21. Migration toward CXCL12 or CCL19 was not affected. These *in vitro* homing assays indicate that multivalent synthetic heparin dendrimers inhibit the migration of lymphocytes toward certain chemokine gradients by blocking the formation of a chemokine concentration gradient on GAG endothelial chains. These findings are in agreement with preliminary *in vivo* measurements of circulating lymphocytes. The results presented here contribute to the understanding of GAG–chemokine interactions, a first step toward the design of novel drugs that modulate chemokine activity.

Chemokines are a family of small, secreted proteins involved in many biological processes such as inflammation or viral infection (*1, 2*). Chemokines induce directed chemotaxis in responsive cells, hence the name *chemo*tactic cyto*kines*. In response to inflammatory stimuli, such as bacterial infection or viruses, chemokines are released from a wide variety of cells and function mainly as chemoattractants for leukocytes, recruiting them from the blood to sites of infection or damage. Some chemokines also play important roles in the immune system as they participate in the migration and arrest of lymphocytes. In order to identify strategies allowing for interference with chemokine function, the molecular mechanisms by which chemokines operate have to be elucidated.

Once secreted, chemokines form a concentration gradient that controls the direction and selectivity of leukocyte cell migration. The interactions of chemokines and G-protein-coupled transmembrane receptors expressed on leukocyte cell surfaces mediate leukocyte migration. In addition, glycosaminoglycans (GAGs) (*3*) are required for chemokines to function *in vivo* (*4*). GAGs are linear, highly sulfated, and heterogeneous polysaccharides that are ubiquitously present on mammalian cell surfaces and within the extracellular matrix. Heparin and heparan sulfate (*5*), chondroitin sulfate, keratan sulfate, dermatan sulfate, and hyaluronic acid are members of the GAG class of carbohydrates. GAGs consist of repeating disaccharide units that differ in the basic monosaccharide sequence, the stereochemistry of the glycosidic linkages, acetylation, and, most importantly, the N- and O-sulfation pattern. Heparin and heparan sulfate are structurally related GAGs, formed by disaccharide repeating units of D-glucosamine (GlcN) and either L-iduronic acid (IdoA) or D-glucuronic acid (GlcA) linked

*Corresponding author, seeberger@org.chem.ethz.ch.

Received for review July 31, 2007 and accepted October 3, 2007.

Published online November 16, 2007

10.1021/cb700159m CCC: $37.00

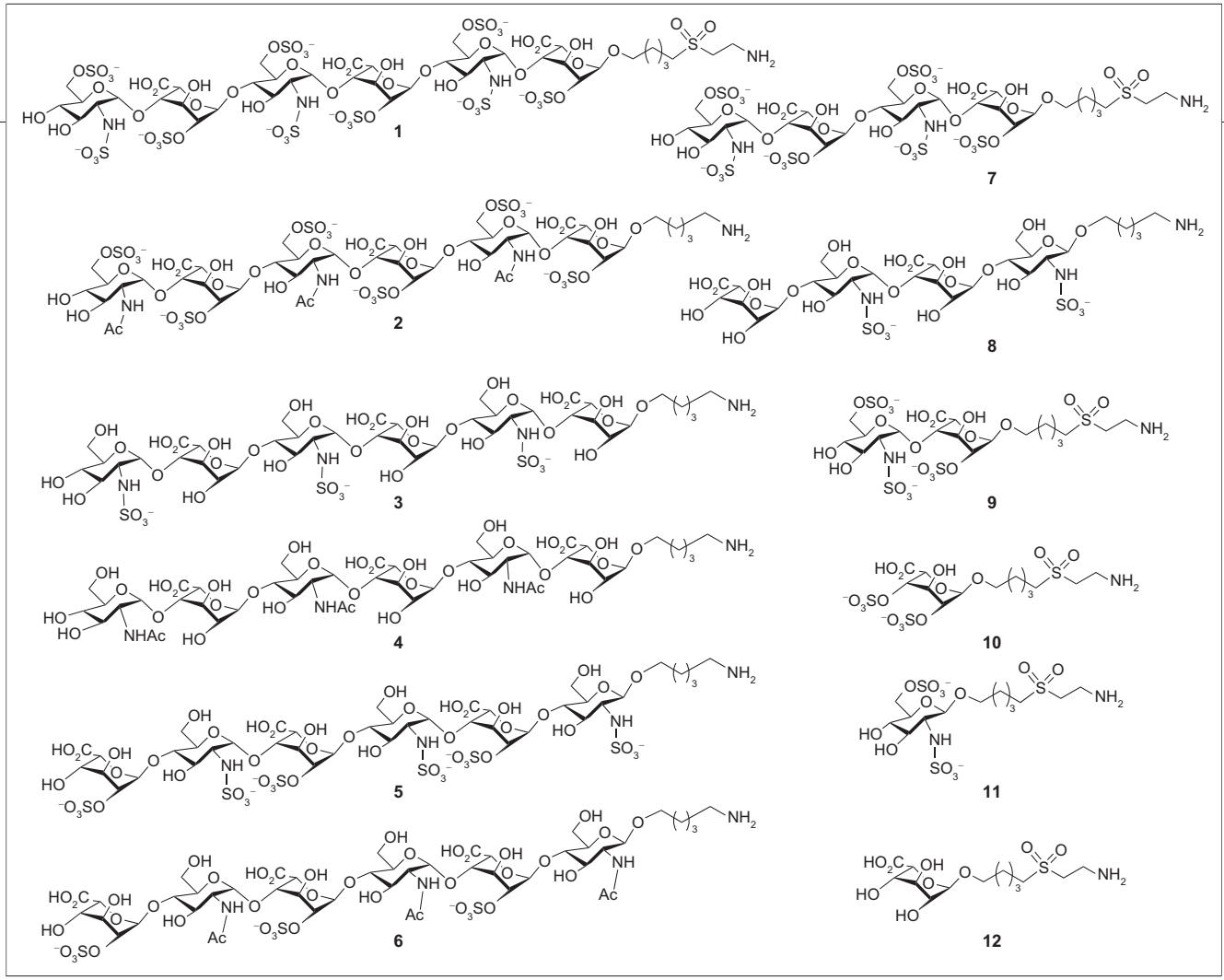

Figure 1. Amine-functionalized heparin oligosaccharides 1–12 employed in the microarray experiments.

via α1–4 and β1–4 glycosidic linkages, respectively. Sulfation can occur at positions 2, 3, and 6 of the GlcN unit and position 2 of IdoA/GlcA. The amino group of the glucosamine residue may also be acetylated or unsubstituted. While heparin is found primarily in mast cells and some hematopoietic cells, as part of the serglycin proteoglycan, heparan sulfate is ubiquitously present on cell surfaces, bound to a variety of core proteins (syndecans, glypicans, perlecan, agrin), and is also a common component of the extracellular matrix, having a broader range of physiological targets than heparin. The uronic acid residues in heparin are more often IdoA (90%) than its C5 epimer GlcA (10%). Moreover, the prototypical heparin disaccharide contains three sulfate groups, rendering heparin one of the most acidic macromolecules in nature (2.7 sulfates per disaccharide on average). On the other hand, heparan sulfate chains are generally longer and more heterogeneous than those of heparin. Heparan sulfate is richer in *N*-acetyl D-glucosamine (GlcNAc) and GlcA units, containing less *O*-sulfates (one sulfate per disaccharide on average).

The conformational flexibility of the pyranose ring of IdoA and the overall helical three-dimensional structure of heparin/heparan sulfate chains increase the chemical complexity of these polysaccharides. Heparins present an astounding level of structural diversity and interact with a wide variety of proteins (*6–10*).

Endothelial heparan sulfate is involved in multiple stages of an *in vivo* inflammatory response (*11*), such as binding and presentation of chemokines at the luminal surface of the endothelium, and in chemokine transcytosis. It is well established that leukocyte subsets can be selectively recruited to inflammatory sites by specific chemokines. It has been hypothesized that heparan sulfate–chemokine interactions (*12*) might control the migration of specific populations of cells and determine which leukocyte subsets enter tissues (*13, 14*). Since the exact composition of GAG chains de-

pends on the type and location of the cell and the pathophysiological state of the tissue and the organism, GAG sequences may also control the activation of specific chemokines.

Oligomerization, required to activate some chemokines, contributes to the complexity of the chemokine activation mechanism and function (*15, 16*). Furthermore, chemokines have the distinct potential to form solid-phase versus soluble gradients that have different functions in the tissue (*17*). Soluble heparin has been shown to reduce inflammation levels by inhibiting the interaction between chemokines and GAGs expressed on the endothelial cell surfaces. However, the clinical use of heparin as anti-inflammatory drug is hampered by the many side effects associated with this molecule including thrombocytopenia. Determining the GAG-binding profiles of chemokines will be a first step for the design of novel heparin mimetics with anti-inflammatory activity and reduced side effects. These molecules would act by blocking the formation of chemokine gradients on cell surfaces.

Carbohydrate microarray technology (*18–24*) has been used recently for the rapid analysis of GAG–protein interactions (*25–32*). Here, we provide some valuable data on the binding affinities of eight chemokines by using heparin chips containing a small library of synthetic heparin oligosaccharides with different sequences and sulfation group distribution (*31*). These chemokines exhibit greatly differing affinities for heparin-like oligosaccharides. This selectivity of chemokine–heparin interaction suggests that cell surface GAGs contribute to the specific activation of chemokines and thereby to the selective recruitment of leukocyte subsets. The study provides structural information to guide the synthesis of molecules aimed at controlling chemokine function. The chip format enabled the characterization of these sugar–protein interactions by using between pico- and femtomoles of both analyte and ligand. The carbohydrate microarray platform is amenable to high-throughput screening of thousands of binding events on a single slide. Surface plasmon resonance (SPR) experiments were employed to validate the array binding results. In addition, *in vitro* homing assays indicate that multivalent dendrimers displaying synthetic GAG sequences inhibit the migration of lymphocytes in the direction of certain chemokine gradients by blocking the formation of a chemokine concentration gradient on endothelial GAG chains.

RESULTS AND DISCUSSION

Screening the Binding Affinities of CCL21, CXCL13, CXCL12, and CCL19 by Carbohydrate Microarrays. We have recently reported the preparation and use of microarrays containing synthetic heparin oligosaccharides (*31*). Briefly, a small library of amine-terminated sugar probes was chemically synthesized (Figure 1) and immobilized on *N*-hydroxysuccinimide (NHS)-activated glass slides by using a robotic DNA printer. A deaminated heparin sample with an average molecular weight of 5 kDa was also included in the microarray experiments as positive control following functionalization with 1,11-diamino-3,6,9-trioxaundecane by reductive amination (*33*). CodeLink slides that are coated with a hydrophilic polymer containing the activated esters gave the highest signal/noise ratios after protein incubation compared with other modes of immobilization: amine-coated glass slides treated with tetraethylene glycol disuccinimidyl disuccinate, aldehyde-coated glass slides, or bovine serum albumin (BSA)-coated slides treated with *N*,*N*′-disuccinimidyl carbonate (*34*). Covalent sugar attachment was demonstrated by comparing amine-terminated heparin oligosaccharides to sugars containing a blocked reducing end. The binding assay involved initial incubation with the heparin-binding protein, followed by detection of the bound protein with a typical sandwich procedure involving primary and fluorescently labeled secondary antibodies.

It is important to note that despite the impressive advances in the synthesis of heparin-like oligosaccharides in the last decades, the preparation of this type of molecule is still challenging. Oligosaccharide structures **1**–**12** were selected based on sulfation patterns (*31*). The library includes oligosaccharides found in heparin/heparan sulfate as well as several "artificial" heparin-like sequences, such as **2**, **6**, and **10**, not found in the natural polymers. For example, hexasaccharide **2** contains the GlcNAc(6-OSO_3)-IdoA(2-OSO_3) repeating unit, not found in heparin since C-5 epimerase does not act on GlcNAc-GlcA sequences during the biosynthetic pathway to heparin/heparan sulfate proteoglycans. Although this synthetic library is limited in number and structural diversity, it still provides useful information on GAG–chemokine recognition.

Initially, we studied four chemokines (CCL21, CXCL13, CXCL12, and CCL19), often regarded as constitutive chemokines, that play a critical role in the immune system by regulating the arrest and recruitment of lym-

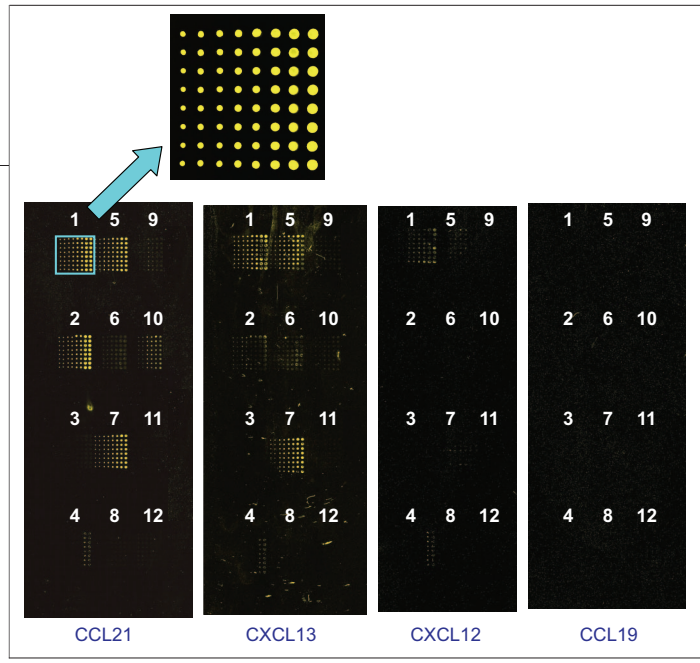

Figure 2. Fluorescence images of heparin microarrays containing oligosaccharides 1–12 probed with CCL21, CXCL13, CXCL12, and CCL19 followed by detection with primary and secondary antibodies. Four different concentrations of sugar solutions, ranging from 16 μM to 2 mM from left to right were employed. All samples were printed in replicates of 16 to produce a microarray containing 768 spots.

phocyte subsets and controlling lymphocyte–endothelial cell recognition (*35, 36*). The microarray screening results obtained for these proteins are shown in Figure 2. Antibodies did not bind spots lacking chemokines. CCL21 (also called Exodus-2) bound to hexasaccharides **1**, **2**, and **5**, tetrasaccharide **7**, and monosaccharide **10** and weakly bound to **6** and **9**. CXCL13, also called BLC, exhibited decreased affinity overall, whereby hexasaccharides **1** and **5** and tetrasaccharide **7** bound best. Interestingly, fluorescent intensities for CCL21 are around 15,000 units while signals for CXCL13 are around 1000 units, using the same chemokine concentration and considering spots with the same sugar concentration (see Figure 3, quantification at 400 μM sugar concentration). These two chemokines are thought to participate in the migration of different lymphocyte subfamilies. CXCL13 strongly attracts B lymphocytes while promoting migration of only small numbers of T cells and macrophages (*36*). On the other hand, CCL21 is a highly efficacious chemoattractant for lymphocytes with preferential activity toward naive T cells (*37*). Migration of lymphocyte subsets, such as B cells, naive T cells, and memory T cells, into different compartments of the secondary lymphoid organs is essential for normal immune function. Our array results suggest that significant overall differences in the chemokine–GAG affinities could be involved in the activation of a specific chemokine and therefore the recruitment of a specific lymphocyte subfamily.

CXCL12 (also called SDF-1α) is a chemoattractant for monocytes and lymphocytes that also inhibits infection of T cells by HIV isolates that use the CXCR4 chemokine receptor (*38*). Binding of CXCL12 to cell surface GAGs has been demonstrated and the heparin-binding site was identified on the crystal structure of the protein (*39, 40*). When CXCL12 was incubated with the heparin chip, we only observed weak binding to hexasaccharide **1**. After incubation with CCL19 (also called MIP-3β), no binding to the synthetic heparin oligosaccharides was detected. Interestingly, CCL21 and CCL19, which differ significantly in their interactions with heparin oligosaccharides, use the same receptor, CCR7. CXCL12 and CCL19 bound, although weakly, to the 5 kDa heparin sample (data not shown), indicating that these two chemokines bind heparin. These results suggest that longer heparin oligosaccharides than those active for CCL21 and CXCL13 or different sulfation patterns not included in our chips are necessary for CXCL12 and CCL19 activation. It could also be hypothesized that GAG binding is not crucial for CXCL12 and CCL19 immobilization on the endothelium.

SPR Measurements Help To Determine Binding Affinities. The heparin microarray experiments indicate that chemokines have different binding affinities for

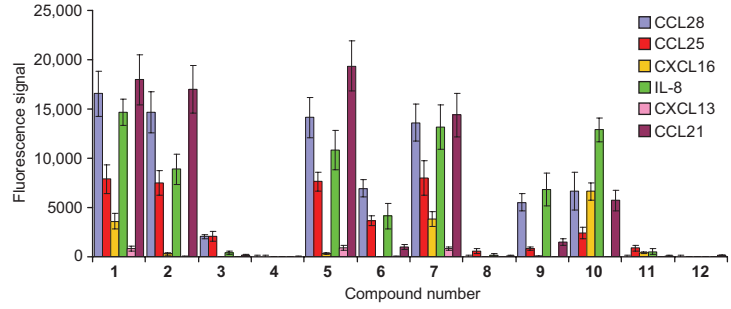

Figure 3. Quantification of the fluorescence signal observed for each immobilized carbohydrate (1–12) after incubation with CCL28, CCL25, CXCL16, IL-8, CXCL13, and CCL21. CXCL12 and CCL19 are not included in the graphic since these two chemokines did not yield significant fluorescent signals above the background. Data presented are the average of 16 spots on the same array at 400 μM sugar concentration; errors are the standard deviations for each measurement.

specific heparin oligosaccharides. CCL21 strongly binds to hexasaccharide **1**, which contains the $GlcNSO_3$(6-OSO_3)-IdoA(2-OSO_3) repeating unit of the major sequence of heparin, while CXCL12 binds only weakly and CCL19 does not bind the hexasaccharide at all. To validate the microarray findings, SPR experiments were conducted. SPR measurements use an optical biosensor that rules out any artifact derived from the primary and secondary antibody staining. The binding affinities of heparin-like oligosaccharides or heparin mimetics are usually measured by using an affinity assay where free ligand competes with immobilized heparin for protein (*41–43*). Heparin or heparan sulfate is usually immobilized onto the sensor chip by biotinylation followed by injection on a streptavidin sensor surface (*44–48*). The use of synthetic amine-functionalized heparin oligosaccharides allowed us to carry out SPR experiments by direct immobilization of the sugar probes on the gold surfaces (*49*).

Hexasaccharide **1** was immobilized on an activated CM5 gold chip by using a 1 mM solution of hexadecyltrimethylammonium chloride. Amide bond formation on a CM5 chip is favored in a low-ionic-strength buffer at a pH below the isoelectric point of the molecule that is immobilized. Under these conditions, the ligand is concentrated on the chip surface by electrostatic attraction between the positively charged ligand and the negatively charged carboxyl groups of the chip (*50*). Immobilization of highly sulfated heparin oligosaccharides such as **1** by amine coupling is difficult since electrostatic preconcentration is not possible due to the presence of negatively charged sulfate groups. The procedure described here overcomes this problem by using positively charged micelles as ligand carriers.

SPR sensorgrams for the binding of chemokines to immobilized **1** (Figure 4) afford additional information on chemokine–heparin interactions in real time. The rising part of each curve corresponds to the association of protein on the chip surface. The final portion of the curves corresponds to the dissociation of protein after the sample volume has finished and the buffer is flowed on the sensor surface again. The SPR findings confirmed the array results. CCL21 bound hexasaccharide **1** best, followed by CXCL13. The dissociation curve for CCL21 is very shallow, indicating a tight interaction. The sensorgram for CXCL12 indicates weak binding as evidenced by a very steep dissociation curve. When CCL19 was flowed over the chip, no significant response was

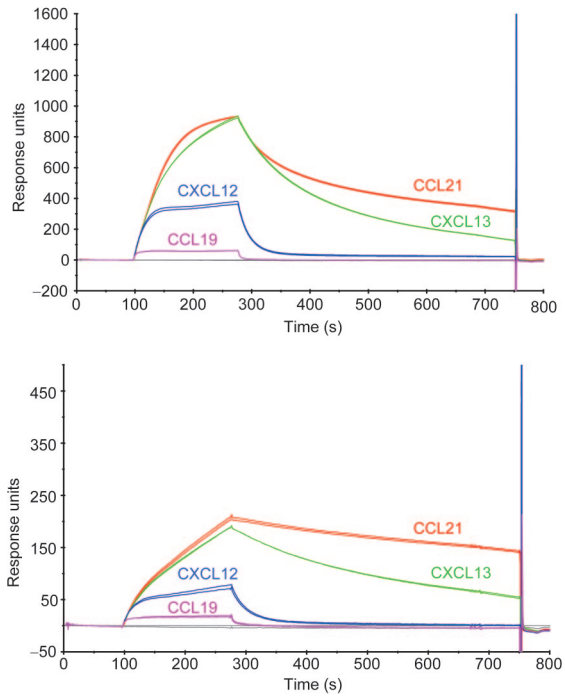

Figure 4. SPR sensorgrams that show the real-time binding of different chemokines to a sensor chip presenting hexasaccharide 1. The protein sample was flowed over the gold surface for 3 min at 100 nM (top) and 25 nM (bottom) in HBS-EP buffer (10 mM HEPES, pH 7.4, 150 mM NaCl, 3 mM EDTA, 0.005% v/v surfactant P20). At the end of the sample injection, the same buffer was flowed over the sensor surface for 6 min to facilitate dissociation. The experiments are shown in duplicate.

observed even when 25 and 100 nM protein solutions were used.

Binding Profiles of IL-8, CCL25, CCL28, and CXCL16. After validating the array protocol by SPR measurements, we determined the binding profiles of four more chemokines: IL-8, CCL25, CCL28, and CXCL16 (Figure 5), three of them (IL-8, CCL28, and CXCL16) are considered inducible chemokines. The prototypic chemokine IL-8 (aka, CXCL8) is mainly involved in the activation and migration of neutrophils (*51, 52*). IL-8 bound sugars **1**, **2**, **5**, **6**, **7**, **9**, and **10**. Comparison of the fluorescence signals for hexasaccharides **3** and **6**, which have the same degree of sulfation, one sulfate group per disaccharide, indicates that binding to the sulfated oligosaccharides is not based on nonspecific charge–charge interactions. Similar conclusions can be drawn from the comparison of the fluorescence signals for monosaccharides **10** and

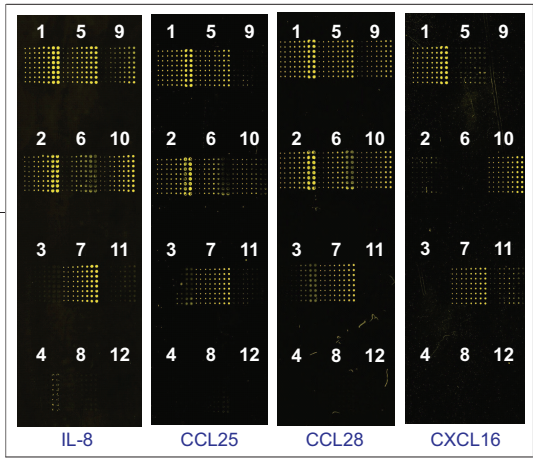

Figure 5. Fluorescence images of heparin microarrays containing oligosaccharides 1–12 probed with IL-8, CCL28, CCL25, and CXCL16 followed by detection with primary and secondary antibodies. Four different concentrations of sugarsolutions, ranging from 16 μM to 2 mM from left to right, were employed. All samples were printed in replicates of 16 to produce a microarray containing 768 spots.

11. Binding to **10** can be explained by the presence of unique, unnatural 2,4-di-O-sulfation pattern. In addition, binding to hexasaccharide **6** suggests that the 2-*O*-sulfate groups at IdoA units play an important role in this interaction. Interestingly, the "artificial" IdoA(2-OSO_3)-GlcNAc sulfation pattern, not present in natural heparin/heparan sulfate, does not activate fibroblast growth factors (FGF)-1, -2, or -4 (*31*). Further studies using more complex libraries of synthetic sugars will be needed to determine the exact structural requirements for IL-8 recognition, ruling out the influence of the disaccharide sequence (GlcN-IdoA for **3**, and IdoA-GlcN for **6**) on the interaction. IL-8 bound oligosaccharides as short as disaccharide **9** and monosaccharide **10**. Conclusions regarding the length of the oligosaccharide required for an interaction should be taking cautiously. Simultaneous protein binding to several immobilized sugar sequences, in a multivalent and cross-linking manner, cannot be entirely ruled out. However, this mode of interaction would be presumably more likely for spots generated with higher sugar concentrations. No significant differences between low and high density spots were observed to support multivalent binding on the plate. Irrespective of the mode of interaction, detection of chemokine binding to small sequences provides interesting information for the design of potential mimetics such as heparin-like glycodendrimers (*33*).

Lindahl et al. (*53*) defined the IL-8-binding domain of heparan sulfate by using naturally derived oligosaccharides and reported that a minimal sequence composed of 18–20 monosaccharide units is required for binding to dimeric IL-8, which is the active form of this protein. This sequence contains two N-sulfated domains of six units, enriched in the trisulfated disaccharide $GlcNSO_3$(6-OSO_3)-IdoA(2-OSO_3) and separated by a fully N-acetylated region. Although variations in the source of oligosaccharides, synthetic vs isolated, may account for these discrepancies, it is also conceivable that the three-dimensional arrangement of sugars on the microarray plates allows for the interaction of short sequences such as disaccharide **9** with the binding sites of each IL-8 monomer in a multivalent and cooperative interaction mode, resulting in IL-8 recognition as proposed in the model introduced by Lindahl.

CCL25 (aka, TECK) (*54*) and CCL28 (aka, MEC) are two closely related epithelial-expressed chemokines, involved in the tissue-specific migration of lymphocytes (*55*). CCL25 attracts dendritic cells, thymocytes, and activated macrophages and is predominantly expressed in the small intestine. Fluorescence signals were detected for **1**, **2**, **5**, and **7**, while **3**, **6**, and **10** were bound less well. CCL28, which is expressed at diverse mucosal sites such as colon and salivary and mammary glands, presents a similar binding profile but with higher overall affinity. CXCL16 is a transmembrane chemokine that regulates movements of activated T cells in the splenic red pulp and in peripheral tissues (*56*). After incubation with CXCL16, binding to compounds **1**, **7**, and **10** was observed.

In summary, the binding profiles (Figure 3) indicate that chemokines have different affinities for heparin oligosaccharides. In general, inducible chemokines show higher affinities than constitutive chemokines. Four of the proteins we tested (CCL21, IL-8, CCL25, and CCL28) bind oligosaccharides **1**, **2**, **5**, and **7** indicating that tetra- and hexasaccharides with at least two sulfate groups per disaccharide constitute a general recognition motif for these chemokines. However, significant differences in the binding affinities are observed when considering shorter and less sulfated sequences such as disaccharide **9**, monosaccharide **10**, or hexasaccharides **3** and **6**. The observation that **6** is generally a better binder than **3** suggests the crucial role of 2-*O*-sulfate groups at IdoA units for this interaction. Interestingly, the CXCL16 binding profile differs significantly with decreased affinity across all structures and monosaccharide **10** as the best binder. Binding was detected for **1** and **7**, which contain the trisulfated repeating unit $GlcNSO_3$(6-OSO_3)-IdoA(2-OSO_3), but not for **2** and **5**, lacking *N*-sulfate and 6-*O*-sulfate groups, respectively, emphasizing the importance of these groups for CXCL16 recognition.

***In Vitro* Chemotaxis Experiments.** *In vitro* chemotaxis experiments were carried out to study the effect of hexasaccharide **1** on lymphocyte migration toward a chemokine gradient. Because human and mouse chemokine protein sequences are highly conserved, we tested the *in vitro* effect of dendrimer binding on murine chemokine activity. Murine splenocytes and lymph

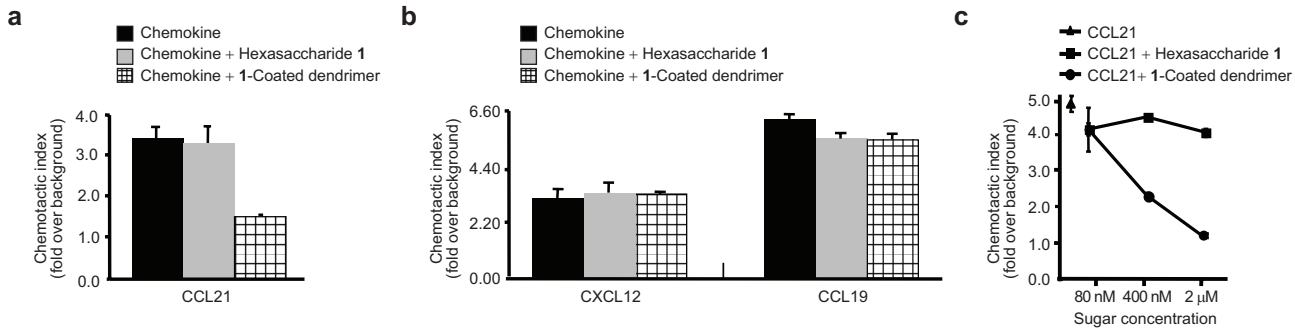

Figure 6. Murine splenocytes and lymph node cells were incubated in transwells above media containing murine chemokine with or without 1 μM hexasaccharide containing compound. CCL21 concentration was 150 nM (panel a), while both CCL19 and CXCL12 were used at 100 nM (panel b). As in panels a and b, lymphocytes were plated in the presence of 150 nM mCCL21 and dilutions of hexasaccharide containing compound (panel c). Quantification of migrated CD3+ cells in the bottom well was compared between groups and displayed as chemotactic index (CD3+ cells that migrated towards chemokine divided by the number of CD3+ cells that migrated without chemokine) where the background migration is 1. Data are representative of experiments with five individual mice in which chemotaxis was analyzed in triplicate wells. The chemotactic response of the total lymphocyte pool was equivalent to those of CD3+ cells (data not shown).

node cells were placed in the upper chambers of transwells, and cell migration toward an optimal concentration of murine CCL21 was quantified by fluorescence activated cell sorting (FACS) (Figure 6, panel a). Results of migration assays are presented as chemotactic index values defined as cell migration toward chemokine divided by the number of cells that migrated without chemokine. CCL21-mediated chemotaxis of the total cell population, and T cells in particular, did not change significantly upon addition of hexasaccharide **1**. However, when a polyamidoamine (PAMAM) dendrimer coated with **1** (*33*) was co-incubated with the chemokine, there was nearly complete inhibition of chemotaxis (Figure 6, panel a) in a dose-dependent manner (Figure 6, panel c). Dendrimers are nanosized, radially symmetric molecules with well-defined, homogeneous, and monodisperse structure consisting of tree-like arms or branches. Dendrimer coated with **1** was prepared by covalent coupling of **1** and generation 2.5 PAMAM dendrimer, which contains 32 carboxylic acid groups. Eight sugars were bound per dendrimer (25% loading) as determined by NMR spectroscopy (*33*). Nonfunctionalized dendrimer did not affect lymphocyte migration. These results indicate that the multivalent display of heparin oligosaccharides enhances their binding capacity by mimicking the naturally occurring cell surface GAG chains. Treatment with multivalent heparin conjugates of defined structure may inhibit leukocyte chemotaxis by displacement of GAG-bound chemokines from the endothelium and extravascular sites of chemokine deposition, blocking the formation of chemokine gradients on cell-surface GAGs. Preliminary *in vivo* assays in mice showed subtle changes of blood cell populations in the presence of dendrimer coated with **1** (data not shown). After intravenous injection of dendrimer, a modest and short-lived increase in the number of circulating lymphocytes was observed in the presence of **1**-coated dendrimer. This effect is likely due to an inability of lymphocytes to stick to the endothelium and enter lymph nodes.

We also investigated the chemotaxis of murine T cells to murine CCL19 and CXCL12 (Figure 6, panel b). According to our microarray results, CCL21 strongly binds to hexasaccharide **1**, while CCL19 does not bind at all and CXCL12 binds only weakly to the hexasaccharide. In agreement with the microarray binding results, hexasaccharide **1** and dendrimer coated with **1** failed to inhibit chemotactic responses toward CCL19 and CXCL12, thus highlighting the selectivity of GAG–chemokine interactions. This finding also may explain the subtle *in vivo* effect of **1**-coated dendrimer on lymphocyte migration since dendrimer coated with **1** is unable to block the effects of CCL19 and CXCL12, which along with CCL21 can also mediate homing to secondary lymphoid organs.

In summary, we prepared microarrays containing synthetic heparin oligosaccharides by using a linker strategy that is compatible with the protecting-group ma-

nipulations (*57–59*) required for the synthesis of the highly sulfated oligosaccharides. We employed these microarrays to provide valuable information about the binding profiles of several chemokines that are implicated in the selective recruitment of lymphocytes and neutrophils and play a crucial role in the immune system, inflammatory processes, and viral infection. The chip format requires only pico- to femtomoles of both analyte and ligand to characterize sugar–protein interactions. Moreover, thousands of binding events can be screened on a single slide, and the number is currently limited only by access to synthetic heparin oligosaccharides. The array data provides important information about the structural requirements for GAG chains needed to enable chemokine recognition. These studies aid the elucidation of chemokine function at the molecular level and the design of novel anti-inflammatory drugs that block chemokine–GAG interactions. The SPR measurements using amine-terminated synthetic sugars directly immobilized on the gold sensor surface validated the array results. *In vitro* chemotaxis assays were used to assess the effect of hexasaccharide **1** on lymphocyte migration mediated by specific chemokines. Treatment with multivalent dendrimers containing **1** strongly reduced cell migration toward CCL21, suggesting an important role of multivalent presentation in GAG–chemokine interactions. Heparin-containing dendrimers are an interesting starting point for the design of chemokine-modulating agents based on well-defined GAG oligosaccharides since they interfere with chemokine function but lack the disadvantages of natural heparin.

METHODS

Materials. All aqueous solutions were made from nanopure water. Solutions used for chip hybridization were sterile filtered through a 0.2 μm syringe filter prior to use. Recombinant human CXCL12, recombinant human CCL19, recombinant human CCL21, recombinant murine CXCL13, recombinant human CCL28, recombinant human CCL25, and recombinant human CXCL16 were purchased from PeproTech EC (London, U.K.). Rabbit anti-human CXCL12 was obtained from Aviva Systems Biology. Polyclonal rabbit anti-mouse CXCL13 was purchased fromeBioscience. Polyclonal rabbit anti-human CCL19 was purchased from Abgent. Goat polyclonal anti-human CCL21 was obtained from Abcam. Goat anti-human CCL28 and CCL25 were obtained from R&D Systems. Rabbit anti-human CXCL16 was purchased from PeproTech EC. Human IL-8 and rabbit anti-human IL-8 were a kind gift of Dr. Antal Rot (Novartis, Austria). Goat anti-rabbit IgG and rabbit anti-goat IgG labeled with Alexa Fluor 546 dye were purchased from Molecular Probes and employed to detect the primary antibodies. CodeLink slides were purchased from Amersham Biosciences. Microarrays were constructed using a Perkin-Elmer noncontact printer. HybriSlip hybridization covers were purchased from Grace BioLabs (Bend, OR). Slides were scanned using a LS400 scanner from Tecan (Männedorf, Switzerland) and quantified using Scan Array Express (Perkin-Elmer) and Gene Spotter (MicroDiscovery GmbH, Berlin, Germany) software. SPR measurements were performed on a BIA-core 3000 (BIAcore, Uppsala, Sweden) operated by the Biacore control software. HBS-EP buffer (10 mM HEPES, pH 7.4, 150 mM NaCl, 3 mM EDTA, 0.005% v/v surfactant P20) and CM5 chips were purchased from BIAcore. Starburst PAMAM dendrimer generation 2.5 containing 32 sodium carboxylate surface groups and deaminated heparin (5 kDa) were purchased from Sigma-Aldrich.

Heparin Microarray Fabrication. Amine-functionalized heparin oligosaccharides **1**–**12** (Figure 1) were prepared as described previously (*25, 31*). Synthetic oligosaccharides were spatially arrayed onto NHS-activated CodeLink slides by use of an automated arraying robot in sodium phosphate buffer (pH 9.0, 50 mM). Slides were printed in 50% relative humidity at 22 °C, followed by incubation overnight in a saturated NaCl chamber that provides an environment of 75% relative humidity. The robot delivered 1 nL of sugar solutions at four different concentrations (2 mM, 400 μM, 80 μM, and 16 μM), and the resulting spots had an average diameter of 200 μm with a distance of 500 μm between the centers of adjacent spots. All samples were printed in replicates of 16. Slides were then washed three times with water to remove the unbound carbohydrates from the surface. Remaining succinimidyl groups were quenched by placing slides in a solution preheated to 50 °C that contained 100 mM ethanolamine in sodium phosphate buffer (pH 9.0, 50 mM) for 1 h. Slides were rinsed several times with distilled water, dried by centrifugation, and stored in a desiccator prior to use.

Microarray Binding Assay. The protein hybridization solutions were prepared by diluting the stock solutions to a concentration of 20 μg mL^{-1} with PBS buffer (pH 7.5, 10 mM) containing BSA (1%). Array incubations were performed as follows: 100 μL of protein solution were placed between array slides and plain coverslips and incubated for 1 h at RT. The arrays were washed with PBS (pH 7.5, 10 mM) containing 1% Tween 20 and 0.1% BSA and twice with water and then centrifuged for 5 min to ensure dryness. For detection of bound chemokines, arrays were incubated with polyclonal rabbit or goat anti-chemokine antibodies (20 μg mL^{-1}) and then washed as described above. Finally, AlexaFluor-546-labeled anti-rabbit or anti-goat IgG (20 μg mL^{-1}) was used to detect bound rabbit or goat primary antibodies, respectively, and washed as above.

Image Acquisition and Signal Processing. Heparin arrays were scanned by using a LS400 scanner, and fluorescence intensities from these scans were integrated on Scan Array Express and Gen Spotter software. Signal to background was typically ≥50:1. The local background was subtracted from the hybridization signal of each separate spot, and the mean intensity of each spot was used for data analysis. Spot finding was automatically performed, followed by manual fitting to correct for spot deviations. Data presented are the average of 16 spots on the same array at 400 μM sugar concentration; errors are the standard deviations for each measurement.

SPR Measurements: Immobilization of Hexasaccharide 1 on a CM5 Sensor Chip. Hexasaccharide **1** was covalently bound to the sensor surface via the terminal primary amino group using the following protocol. HBS-EP was employed as running buffer.

The carboxymethylated dextran matrix (CM5 chip) was first activated at a flow rate of 5 μL min^{-1} by using a 15 min (75 μL) injection pulse of an aqueous solution containing NHS (0.05 M) and *N*-ethyl-*N*′-(dimethylaminopropyl) carbodiimide (EDC, 0.2 M). Next, a 50 μL injection of **1** (500 μg mL^{-1}) in 5 mM sodium phosphate buffer (pH 7.4) containing 1 M NaCl was flowed over the activated surface followed by an additional 50 μL injection of **1** (500 μg mL^{-1}) in 5 mM sodium phosphate buffer (pH 7.4) containing 1 mM hexadecyltrimethylammonium chloride. Remaining activated sites on the chip surface were blocked with a 35 μL injection of 1 M ethanolamine hydrochloride solution (pH 8.5). A second flow cell of the CM5 chip was used as negative control after activation with EDC and NHS followed by treatment with ethanolamine solution as described above. An increase of approximately 300 response units (RU) was detected in the flow cell containing **1** when compared with the control cell.

Measurement of Chemokine–Hexasaccharide 1 Interactions on Gold Chips. A 30 μL injection of chemokine solution (25 nM and 100 nM in HBS-EP buffer) was made at a flow rate of 10 μL min^{-1}. At the end of the sample injection, the same buffer was flowed over the sensor surface for 6 min to facilitate dissociation. Then, the chip surface was regenerated for the next sample by injecting a 50 μL pulse of 4 M NaCl at 50 μL min^{-1}. The response was monitored as a function of time to result in a sensorgram. All experiments were carried out at least in duplicate.

Chemotaxis Assay. Spleen and lymph node cells (5×10^5 cells) obtained from 6–8 week old C57BL/6 mice were seeded onto 5.0 μm pore Transwell inserts (Costar, Corning Inc.) in a 24-well plate Falcon tissue culture dish in 100 μL of Dulbecco's modified Eagle's medium (DMEM) supplemented with 2% fetal bovine serum (FBS). The lower chamber was filled with 0.6 mL of DMEM supplemented with 2% FBS containing either recombinant murine CXCL12, recombinant murine CCL21, or murine CCL19 (R&D Systems) at the indicated concentrations. Cultures were carried out in an humidified incubator at 37 °C and 5% CO_2 for 2 h. At that time, transwell inserts were removed, and the media from the bottom well was collected for immunostaining. Collected cells were stained in PBS with 2% FBS and 20 mM EDTA. Anti-mouse CD3 was obtained from BD Pharmingen. Samples were resuspended in identical volumes and events acquired for 1 min on a FACSCanto (BDBiosciences).

Acknowledgment: This work was supported by ETH Zürich, Harvard Medical School, and the European Commission (Marie Curie Fellowship for J.L.P.). We thank Dr. A. Rot (Novartis Institutes for BioMedical Research, Vienna, Austria) for kindly supplying human IL-8 and rabbit anti-human IL-8. We thank Dr. J. Sobek (Functional Genomics Center, Zürich) for assistance in the construction of microarrays and M. Scott (Functional Genomics Center, Zürich) for assistance in the SPR measurements.

REFERENCES

1. Rot, A., and von Andrian, U. H. (2004) Chemokines in innate and adaptive host defense: Basic chemokinese grammar for immune cells, *Annu. Rev. Immunol. 22*, 891–928.
2. Rot, A. (1992) Endothelial-cell binding of Nap-1/Il-8 - role in neutrophil emigration, *Immunol. Today 13*, 291–294.
3. Esko, J. D., and Selleck, S. B. (2002) Order out of chaos: Assembly of ligand binding sites in heparan sulfate, *Annu. Rev. Biochem. 71*, 435–471.
4. Handel, T. M., Johnson, Z., Crown, S. E., Lau, E. K., Sweeney, M., and Proudfoot, A. E. (2005) Regulation of protein function by glycosaminoglycans - as exemplified by chemokines, *Annu. Rev. Biochem. 74*, 385–410.
5. Casu, B., and Lindahl, U. (2001) Structure and biological interactions of heparin and heparan sulphate, *Adv. Carbohydr. Chem. Biochem. 57*, 159–206.
6. Capila, I., and Linhardt, R. J. (2002) Heparin - protein interactions, *Angew. Chem., Int. Ed. 41*, 391–412.
7. Noti, C., and Seeberger, P. H. (2005) Chemical approaches to define the structure-activity relationship of heparin-like glycosaminoglycans, *Chem. Biol. 12*, 731–756.
8. Raman, R., Sasisekharan, V., and Sasisekharan, R. (2005) Structural insights into biological roles of protein-glycosaminoglycan interactions, *Chem. Biol. 12*, 267–277.
9. Petitou, M., and van Boeckel, C. A. A. (2004) A synthetic antithrombin III binding pentasaccharide is now a drug! What comes next? *Angew. Chem., Int. Ed. 43*, 3118–3133.
10. Powell, A. K., Yates, E. A., Fernig, D. G., and Turnbull, J. E. (2004) Interactions of heparin/heparan sulfate with proteins: Appraisal of structural factors and experimental approaches, *Glycobiology 14*, 17R–30R.
11. Wang, L. C., Fuster, M., Sriramarao, P., and Esko, J. D. (2005) Endothelial heparan sulfate deficiency impairs L-selectin- and chemokine-mediated neutrophil trafficking during inflammatory responses, *Nat. Immunol. 6*, 902–910.
12. Lortat-Jacob, H., Grosdidier, A., and Imberty, A. (2002) Structural diversity of heparan sulfate binding domains in chemokines, *Proc. Natl. Acad. Sci. U.S.A. 99*, 1229–1234.
13. Parish, C. R. (2005) Heparan sulfate and inflammation, *Nat. Immunol. 6*, 861–862.
14. Kuschert, G. S. V., Coulin, F., Power, C. A., Proudfoot, A. E. I., Hubbard, R. E., Hoogewerf, A. J., and Wells, T. N. C. (1999) Glycosaminoglycans interact selectively with chemokines and modulate receptor binding and cellular responses, *Biochemistry 38*, 12959–12968.
15. Yu, Y. H., Sweeney, M. D., Saad, O. M., Crown, S. E., Handel, T. M., and Leary, J. A. (2005) Chemokine-glycosaminoglycan binding - specificity for CCR2 ligand binding to highly sulfated oligosaccharides using FTICR mass spectrometry, *J. Biol. Chem. 280*, 32200–32208.
16. Proudfoot, A. E. I., Handel, T. M., Johnson, Z., Lau, E. K., LiWang, P., Clark-Lewis, I., Borlat, F., Wells, T. N. C., and Kosco-Vilbois, M. H. (2003) Glycosaminoglycan binding and oligomerization are essential for the in vivo activity of certain chemokines, *Proc. Natl. Acad. Sci. U.S.A. 100*, 1885–1890.
17. Patel, D. D., Koopmann, W., Imai, T., Whichard, L. P., Yoshie, O., and Krangel, M. S. (2001) Chemokines have diverse abilities to form solid phase gradients, *Clin. Immunol. 99*, 43–52.
18. Love, K. R., and Seeberger, P. H. (2002) Carbohydrate arrays as tools for glycomics, *Angew. Chem., Int. Ed. 41*, 3583–3586.
19. Shin, I., Park, S., and Lee, M. R. (2005) Carbohydrate microarrays: An advanced technology for functional studies of glycans, *Chem. Eur. J. 11*, 2894–2901.
20. Mellet, C. O., and Fernandez, J. M. G. (2002) Carbohydrate microarrays, *ChemBioChem 3*, 819–822.
21. Feizi, T., Fazio, F., Chai, W. C., and Wong, C. H. (2003) Carbohydrate microarrays - a new set of technologies at the frontiers of glycomics, *Curr. Opin. Struct. Biol. 13*, 637–645.
22. de Paz, J. L., and Seeberger, P. H. (2006) Recent advances in carbohydrate microarrays, *QSAR Comb. Sci. 25*, 1027–1032.
23. Timmer, M. S. M., Stocker, B. L., and Seeberger, P. H. (2007) Probing glycomics, *Curr. Opin. Chem. Biol. 11*, 59–65.
24. Brun, M. A., Disney, M. D., and Seeberger, P. H. (2006) Miniaturization of microwave-assisted carbohydrate functionalization to create oligosaccharide microarrays, *ChemBioChem 7*, 421–424.
25. de Paz, J. L., Noti, C., and Seeberger, P. H. (2006) Microarrays of synthetic heparin oligosaccharides, *J. Am. Chem. Soc. 128*, 2766–2767.

26. de Paz, J. L., Spillmann, D., and Seeberger, P. H. (2006) Microarrays of heparin oligosaccharides obtained by nitrous acid depolymerization of isolated heparin, *Chem. Commun.* 3116–3118.
27. Zhi, Z. L., Powell, A. K., and Turnbull, J. E. (2006) Fabrication of carbohydrate microarrays on gold surfaces: Direct attachment of nonderivatized oligosaccharides to hydrazide-modified self-assembled monolayers, *Anal. Chem. 78*, 4786–4793.
28. Gama, C. I., Tully, S. E., Sotogaku, N., Clark, P. M., Rawat, M., Vaidehi, N., Goddard, W. A., Nishi, A., and Hsieh-Wilson, L. C. (2006) Sulfation patterns of glycosaminoglycans encode molecular recognition and activity, *Nat. Chem. Biol. 2*, 467–473.
29. Yamaguchi, K., Tamaki, H., and Fukui, S. (2006) Detection of oligosaccharide ligands for hepatocyte growth factor/scatter factor (HGF/SF), keratinocyte growth factor (KGF/FGF-7),RANTES, and heparin cofactor II by neoglycolipid microarrays of glycosaminoglycan-derived oligosaccharide fragments, *Glycoconjugate J. 23*, 513–523.
30. Shipp, E. L., and Hsieh-Wilson, L. C. (2007) Profiling the sulfation specificities of glycosaminoglycan interactions with growth factors and chemotactic proteins using microarrays, *Chem. Biol. 14*, 195–208.
31. Noti, C., de Paz, J. L., Polito, L., and Seeberger, P. H. (2006) Preparation and use of microarrays containing synthetic heparin oligosaccharides for the rapid analysis of heparin-protein interactions, *Chem.—Eur. J. 12*, 8664–8686.
32. de Paz, J. L., Horlacher, T., and Seeberger, P. H. (2006) Oligosaccharide microarrays to map interactions of carbohydrates in biological systems, *Methods Enzymol. 415*, 269–292.
33. de Paz, J. L., Noti, C., Böhm, F., Werner, S., and Seeberger, P. H. (2007) Potentiation of fibroblast growth factor activity by synthetic heparin oligosaccharide glycodendrimers, *Chem. Biol. 14*, 879–887.
34. Disney, M. D., and Seeberger, P. H. (2004) Aminoglycoside microarrays to explore interactions of antibiotics with RNAs and proteins, *Chem.—Eur. J. 10*, 3308–3314.
35. Campbell, J. J., Hedrick, J., Zlotnik, A., Siani, M. A., Thompson, D. A., and Butcher, E. C. (1998) Chemokines and the arrest of lymphocytes rolling under flow conditions, *Science 279*, 381–384.
36. Gunn, M. D., Ngo, V. N., Ansel, K. M., Ekland, E. H., Cyster, J. G., and Williams, L. T. (1998) A B-cell-homing chemokine made in lymphoid follicles activates Burkitt's lymphoma receptor-1, *Nature 391*, 799–803.
37. Gunn, M. D., Tangemann, K., Tam, C., Cyster, J. G., Rosen, S. D., and Williams, L. T. 1998A chemokine expressed in lymphoid high endothelial venules promotes the adhesion and chemotaxis of naive T lymphocytes, *Proc. Natl. Acad. Sci. U.S.A. 95*, 258–263.
38. Oberlin, E., Amara, A., Bachelerie, F., Bessia, C., Virelizier, J. L., ArenzanaSeisdedos, F., Schwartz, O., Heard, J. M., ClarkLewis, I., Legler, D. F., Loetscher, M., Baggiolini, M., and Moser, B. (1996) The CXC chemokine SDF-1 is the ligand for LESTR/fusin and prevents infection by T-cell-line-adapted HIV-1, *Nature 382*, 833–835.
39. Sadir, R., Baleux, F., Grosdidier, A., Imberty, A., and Lortat-Jacob, H. (2001) Characterization of the stromal cell-derived factor-l alpha-heparin complex, *J. Biol. Chem. 276*, 8288–8296.
40. Mbemba, E., Gluckman, J. C., and Gattegno, L. (2000) Glycan and glycosaminoglycan binding properties of stromal cell-derived factor (SDF)-1 alpha, *Glycobiology 10*, 21–29.
41. Cochran, S., Li, C. P., Fairweather, J. K., Kett, W. C., Coombe, D. R., and Ferro, V. (2003) Probing the interactions of phosphosulfomannans with angiogenic growth factors by surface plasmon resonance, *J. Med. Chem. 46*, 4601–4608.
42. Freeman, C., Liu, L. G., Banwell, M. G., Brown, K. J., Bezos, A., Ferro, V., and Parish, C. R. (2005) Use of sulfated linked cyclitols as heparan sulfate mimetics to probe the heparin/heparan sulfate binding specificity of proteins, *J. Biol. Chem. 280*, 8842–8849.
43. Cochran, S., Li, C. P., and Bytheway, I. (2005) An experimental and molecular-modeling study of the binding of linked sulfated tetracyclitols to FGF-1 and FGF-2, *ChemBioChem 6*, 1882–1890.
44. Capila, I., VanderNoot, V. A., Mealy, T. R., Seaton, B. A., and Linhardt, R. J. (1999) Interaction of heparin with annexin V, *FEBS Lett. 446*, 327–330.
45. Hernaiz, M., Liu, J., Rosenberg, R. D., and Linhardt, R. J. (2000) Enzymatic modification of heparan sulfate on a biochip promotes its interaction with antithrombin III, *Biochem. Biophys. Res. Commun. 276*, 292–297.
46. Caldwell, E. E. O., Andreasen, A. M., Blietz, M. A., Serrahn, J. N., VanderNoot, V., Park, Y., Yu, G. Y., Linhardt, R. J., and Weiler, J. M. (1999) Heparin binding and augmentation of C1 inhibitor activity, *Arch. Biochem. Biophys. 361*, 215–222.
47. Lubineau, A., Lortat-Jacob, H., Gavard, O., Sarrazin, S., and Bonnaffe, D. (2004) Synthesis of tailor-made glycoconjugate mimetics of heparan sulfate that bind IFN-gamma in the nanomolar range, *Chem.—Eur. J. 10*, 4265–4282.
48. Guerrini, M., Agulles, T., Bisio, A., Hricovini, M., Lay, L., Naggi, A., Poletti, L., Sturiale, L., Torri, G., and Casu, B. (2002) Minimal heparin/heparan sulfate sequences for binding to fibroblast growth factor-1, *Biochem. Biophys. Res. Commun. 292*, 222–230.
49. Suda, Y., Arano, A., Fukui, Y., Koshida, S., Wakao, M., Nishimura, T., Kusumoto, S., and Sobel, M. (2006) Immobilization and clustering of structurally defined oligosaccharides for sugar chips: An improved method for surface plasmon resonance analysis of protein-carbohydrate interactions, *Bioconjugate Chem. 17*, 1125–1135.
50. Johnsson, B., Lofas, S., and Lindquist, G. (1991) Immobilization of proteins to a carboxymethyldextran-modified gold surface for biospecific interaction analysis in surface-plasmon resonance sensors, *Anal. Biochem. 198*, 268–277.
51. Middleton, J., Neil, S., Wintle, J., ClarkLewis, I., Moore, H., Lam, C., Auer, M., Hub, E., and Rot, A. (1997) Transcytosis and surface presentation of IL-8 by venular endothelial cells, *Cell 91*, 385–395.
52. Webb, L. M. C., Ehrengruber, M. U., Clarklewis, I., Baggiolini, M., and Rot, A. (1993) Binding to heparan-sulfate or heparin enhances neutrophil responses to interleukin-8, *Proc. Natl. Acad. Sci. U.S.A. 90*, 7158–7162.
53. Spillmann, D., Witt, D., and Lindahl, U. (1998) Defining the interleukin-8-binding domain of heparan sulphate, *J. Biol. Chem. 273*, 15487–15493.
54. Zaballos, A., Gutierrez, J., Varona, R., Ardavin, C., and Marquez, G. (1999) Cutting edge: Identification of the orphan chemokine receptor GPR-9-6 as CCR9, the receptor chemokine TECK, *J. Immunol. 162*, 5671–5675.
55. Kunkel, E. J., and Butcher, E. C. (2002) Chemokines and the tissue-specific migration of lymphocytes, *Immunity 16*, 1–4.
56. Matloubian, M., David, A., Engel, S., Ryan, J. E., and Cyster, J. G. (2000) A transmembrane CXC chemokine is a ligand for HIV-coreceptor Bonzo, *Nat. Immunol. 1*, 298–304.
57. Orgueira, H. A., Bartolozzi, A., Schell, P., Litjens, R., Palmacci, E. R., and Seeberger, P. H. (2003) Modular synthesis of heparin oligosaccharides, *Chem. Eur. J. 9*, 140–169.
58. de Paz, J. L., and Martin-Lomas, M. (2005) Synthesis and biological evaluation of a heparin-like hexasaccharide with the structural motifs for binding to FGF and FGFR, *Eur. J. Org. Chem.* 1849–1858.
59. de Paz, J. L., Ojeda, R., Reichardt, N., and Martin-Lomas, M. (2003) Some key experimental features of a modular synthesis of heparin-like oligosaccharides, *Eur. J. Org. Chem.* 3308–3324.